CHEMISTRY
A EUROPEAN JOURNAL

DOI: 10.1002/chem.200802028

Molecular Self-Recognition: Rotational Spectra of the Dimeric 2-Fluoroethanol Conformers

Xunchen Liu, Nicole Borho, and Yunjie Xu*[a]

Abstract: Fluoroalcohols show competitive formation of intra- and intermolecular hydrogen bonds, a property that may be crucial for the protein-altering process in a fluoroalcohol/water solution. In this study, we examine the intra- and intermolecular interactions of 2-fluoroethanol (FE) in its dimeric conformers by using rotational spectroscopy and ab initio calculations. Three pairs of homo- and heterochiral dimeric FE conformers are predicted to be local minima at the MP2/6-311++G(d,p) level of theory. They are solely made of the slightly distorted most stable $G+g-/G-g+$ FE monomer units. Jet-cooled rotational spectra of four out of the six predicted dimeric conformers were observed and unambiguously assigned for the first time. All four observed dimeric conformers have compact geometries in which the fluoromethyl group of the acceptor tilts towards the donor and ensures a large contact area. Experimentally, the insertion of the O–H group of one FE subunit into the intramolecular O–H···F bond of the other was found to lead to a higher stabilisation than the pure association through an intermolecular O–H···O–H link. The hetero- and homochiral combinations were observed to be preferred in the inserted and the associated dimeric conformers, respectively. The experimental rotational constants and the stability ordering are compared with the ab initio calculations at the MP2 level with the 6-311++G(d,p) and aug-cc-pVTZ basis sets. The effects of fluorination and the competing inter- and intramolecular hydrogen bonds on the stability of the dimeric FE conformers are discussed.

Keywords: fluorine · hydrogen bonds · molecular complexes · rotational spectroscopy

Introduction

Fluoroalcohols can alter the secondary and tertiary substructures of proteins and polypeptides when used as a cosolvent in aqueous solutions.[1,2] NMR spectroscopy,[3] X-ray diffraction,[4] circular dichroism,[5] FTIR spectroscopy[6] and molecular dynamics approaches[7] have enriched our understanding of the mechanism of the fluoroalcohol intervention in peptide binding. A detailed picture of this important process, on the other hand, is still lacking. A prerequisite for the understanding of protein–ligand interactions is the precise knowledge of the physical properties of the fluoroalcohol solvent and the aqueous solution themselves.[8,9] It has been proposed that small fluoroalcohol aggregates are crucial for the protein altering process.[10] Suhm and co-workers had recently used a bottom-up approach to tackle the question of intermolecular binding in fluoroalcohol solvents. They investigated small clusters of trifluoroethanol[11,12] and 2-fluoroethanol (FE)[13] produced in a molecular expansion by means of low-resolution IR and Raman spectroscopy, enhanced by molecular modelling and quantum chemical approaches. In the FE study, they tentatively identified four dimeric FE conformers based on the observed and calculated vibrational contours and the "Argon (Ar) test",[14] in which a small amount of Ar is added to the free jet expansion of Helium (He) to promote collisional relaxation and to convert the higher-lying conformers to the global minimum structure. The method of broadband jet FTIR spectroscopy has the advantage of providing an overview of the vibrational band contour patterns of the hydrogen-bonded aggregates with good signal-to-noise ratios and high reproducibility. This low-resolution method, on the other hand, does not provide direct structural information. Such information is extracted in an indirect way through the analysis of the vibrational frequencies, together with pressure dependence and isotopic studies and theoretical calculations. It is therefore desirable to probe the fluoroalcohol aggregates by using high-resolution spectroscopic techniques for which

[a] X. Liu, Dr. N. Borho, Prof. Dr. Y. Xu
Department of Chemistry
University of Alberta
Edmonton, AB, T6G 2G2 (Canada)
Fax: (+1) 780-492-8231
E-mail: yunjie.xu@ualberta.ca

Supporting information for this article is available on the WWW under http://dx.doi.org/10.1002/chem.200802028.

each individual conformer can be unambiguously identified with its own set of rotational constants. These small aliphatic systems are inaccessible to the sensitive fluorescence spectroscopic techniques, previously applied in the pioneering work in chiral recognition by Zenhacker and co-workers, because they lack an aromatic chromophore. One suitable method is Fourier transform microwave (FTMW) spectroscopy, which is known to offer highly accurate structural information. It has been applied in recent years to characterise large and biologically relevant systems such as phenylglycine,[15] the ethanol dimer[16] and molecular lock and key model systems.[17,18] Furthermore, this technique can profit from the generous dipole moments of the fluoro-containing organic compounds in the excitation and emission detection processes.

In this paper, we present the assignments and the analyses of rotational spectra of four dimeric FE conformers, by using FTMW spectroscopy, complemented with high-level ab initio calculations. The stability ordering of the four coexisting dimeric FE conformers was established by monitoring their transition intensities in a conexpansion of FE and Neon (Ne) and by performing the "Ar test". The experimental data of the rotational constants, the magnitudes of the electric dipole moment components, and the stability ordering are compared with the ab initio predictions. The effects of fluorination and the competing inter- and intramolecular hydrogen bonds on the stability of the conformers of the FE dimer are discussed.

Results

Preliminary model calculations: Ab initio geometry predictions of the targeted complexes, although not essential, are of great help for spectral assignments, especially when large numbers of conformers are anticipated. In addition to the rotational constants, the calculations can also provide information about the electric dipole moment components and the preliminary relative stabilities of the possible conformers. Ab initio calculations were performed using the second-order Møller–Plesset (MP2) perturbation theory[19] with the 6-311++G(d,p) basis set.[20] The MP2/6-311++G(d,p) level of theory was chosen because it provided astonishingly good agreement between the predicted and the experimentally observed geometries for several van der Waals[21] and hydrogen-bonded complexes[22] in a number of previous studies.

The FE monomer has two structurally relevant dihedral angles: τ(FCCO) and τ(CCOH). Each can adopt three values of approximately 0° (*trans* or *t*/*T*), +60° (*gauche*+ or *g*+/*G*+), and −60° (*gauche*− or *g*−/*G*−). This leads to nine possible combinations with four mirror image or enantiomeric pairs: *G*+*g*−/*G*−*g*+, *G*+*g*+/*G*−*g*−, *G*+*t*/*G*−*t*, *Tg*−/*Tg*+, and *Tt*—the capital letters represent the conformation of τ(FCCO) and the lower case that of τ(CCOH). The Newman projections of these nine combinations are given in Figure S1 and the relative energy ordering of them and the Cartesian coordinates of the *G*+*g*− conformer are given in Table S1 and S2, respectively, in the Supporting Information. Based on the MP2/6-311++G(d,p) calculations, the *G*+*g*−/*G*−*g*+ pair is more stable by 7 kJ mol^{-1} compared to the next higher energy conformer. This is consistent with the previous experimental and theoretical studies,[13,23,24] showing that the *G*+*g*−/*G*−*g*+ pair is by far the dominant conformations.

The two species of an enantiomeric pair of FE have the same energy and the same rotational spectrum without considering the possible minute effect of parity violation. However, in a chiral environment, for example, when binding to FE itself, the two chiral forms of FE interact differently, resulting in different binding energies. This subtle chirality recognition is taken into account in the initial search of the dimeric FE conformers. The dimeric FE conformers are expected to be linked by an intermolecular O–H···O–H bond. To identify the low energy dimeric conformers that are relevant in a free jet expansion, Scharge et al.[13] carried out initial screening calculations at the HF/3-21G and HF/3-21G* levels and additional calculations at the MP2/6-31+G(d) and MP2/6-311+G(d) levels for the six lowest energy conformers. The nine monomeric conformers are expected to generate 81 dimeric combinations, without considering the more subtle differences in the secondary hydrogen bonds in each combination. Our further exploratory calculations at the MP2/6-311++G(d,p) level point to the same conclusion: the most stable dimeric FE conformers are formed by the *G*+*g*−/*G*−*g*+ FE monomer subunits, and the next most stable group of dimeric conformers, which are complexes composed of the *G*+*g*−/*G*−*g*+ and *G*+*g*+/*G*−*g*− subunits and of the *G*+*g*−/*G*−*g*+ and *Tt* subunits, are about 5–10 kJ mol^{-1} higher in energy than the most stable one. The dimeric FE conformers with only an O–H···F intermolecular hydrogen bond have also been surveyed. These are 6–9 kJ mol^{-1} less stable than the global minimum structure.

In the following, we focus on the four combinations formed by the *G*+*g*−/*G*−*g*+ FE subunits, namely *G*+*g*−→*G*+*g*−, *G*+*g*−→*G*−*g*+, *G*−*g*+→*G*+*g*−, and *G*−*g*+→*G*−*g*+, with the arrow indicating the hydrogen-bond-donating direction. These four can be classified as homochiral (*hom*) or heterochiral (*het*) complexes based on the chirality of the two binding subunits. The two *hom* configurations are mirror images to each other, as are the two *het* ones. Since rotational spectroscopy cannot tell apart the two mirror images, we end up with only two distinguishable conformers: *hom* and *het*. For simplicity, we choose to use *G*+*g*− as the hydrogen-bond acceptor throughout this paper. When forming the O–H···O–H intermolecular hydrogen bond, the hydroxyl group of the donor can either be inserted into the intramolecular O–H···F five-membered hydrogen-bond ring or simply associated to the hydroxyl group of the acceptor. While the inserted (*i*) conformers have a seven-membered ring with the consecutive O–H···O and O–H···F hydrogen bonds, the associated (*a*) conformers leave the intramolecular O–H···F five-membered hydrogen-bond

ring of the acceptor intact. A further consideration is that the hydrogen donor can either bind to the right- or left-hand lone pair of the oxygen atom of the acceptor. This gives rise to two different relative orientations of the two binding partners. One of them is compact (c), with the fluoromethyl group of the acceptor tilting towards the donor, ensuring a large contact area. The other is open (o), with the fluoromethyl group of the acceptor pointing away from the donor. Therefore, we expect $2^3=8$ conformers. Each conformer is named using the three abbreviations of the structural properties. For example, $i|c|het$ means that the conformer has an inserted intermolecular hydrogen-bond ring, with the two binding partners in the compact relative orientation, and is heterochiral. This labelling scheme is the same as that used in reference [13].

Six out of the eight structures proposed above were confirmed to be true minima by the ab initio calculations, while two of them, namely $a|o|hom$ and $a|o|het$, are saddle points. These conformers are summarised in Figure 1 with their important intermolecular distances. Side views of the geometries of the six conformers are given in Figure S2 and their Cartesian coordinates are shown in Table S3, available as Supporting Information. The side views provide better visual discrimination between the compact and open conformers. The raw, zero-point energy (ZPE), and basis set superposition error (BSSE)[25] corrected energy values are listed in Table 1, together with the predicted rotational constants and the dipole moment components of the six conformers.

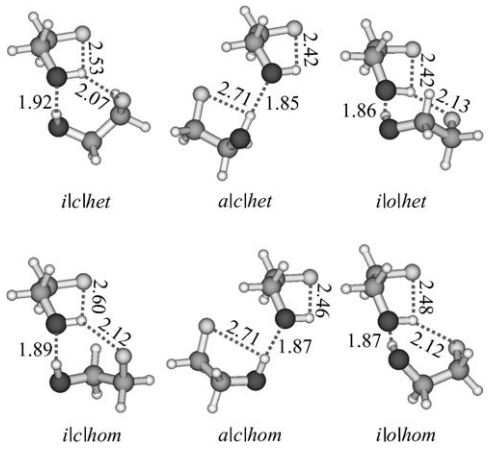

Figure 1. Optimised geometries of the six dimeric FE conformers at the MP2/6-311++G(d,p) level of theory. The important intra- and intermolecular bond distances are indicated in units of Å.

Assignment of the FE dimer rotational spectra: The energy span among the six dimeric conformers is about 2 kJ mol^{-1} at the MP2/6-311++G(d,p) level. Each conformer has at least one substantial dipole-moment component. Therefore, one may expect to observe all six conformers in a supersonic jet expansion. The expansion of 0.3% FE in Ne carrier gas generates many species. Besides the targeted dimeric FE conformers, there are also the conformers of the FE monomer, other small FE oligomers and the FE···Ne$_x$ van der Waals complexes. The rotational spectrum of the dominating $G+g-/G-g+$ conformations of the FE monomer was reported previously.[23,24,26] The known FE transitions were

Table 1. Calculated raw (D_e) and ZPE-corrected (D_0) dissociation energies, rotational constants, and the magnitudes of the electric dipole moment components of the six most stable hydrogen bonded dimeric FE conformers at the MP2/6-311++G(d,p), MP2/aug-cc-pVTZ//MP2/6-311++G(d,p), and MP2/aug-cc-pVTZ level of theory.

	$i\|c\|het$	$i\|c\|hom$	$a\|c\|het$	$a\|c\|hom$	$i\|o\|het$	$i\|o\|hom$
MP2/6-311++G(d,p)						
D_e[a] [kJmol^{-1}]	34.81 (22.96)	33.92 (22.14)	34.00 (23.83)	33.75 (23.54)	32.26 (22.77)	33.20 (23.45)
D_0[a] [kJmol^{-1}]	30.00 (18.14)	29.26 (17.48)	29.89 (19.72)	29.60 (19.38)	27.92 (18.43)	28.59 (18.84)
$\|\mu_a\|$[b] [D]	0.54 (0.53)	1.33 (1.35)	0.06 (0.21)	0.67 (1.00)	0.82 (0.71)	0.69 (0.57)
$\|\mu_b\|$ [D]	0.44 (0.35)	0.77 (0.95)	2.07 (2.27)	1.81 (1.99)	0.33 (0.50)	0.31 (0.47)
$\|\mu_c\|$ [D]	0.78 (0.96)	0.92 (0.86)	0.09 (0.05)	1.51 (1.61)	1.45 (1.53)	0.31 (0.34)
A [MHz]	2477	2498	2905	2869	3239	3287
B [MHz]	1110	1016	872	880	762	761
C [MHz]	1033	1010	765	785	645	642
MP2/aug-cc-pVTZ//MP2/6-311++G(d,p)[c]						
D_e[a] [kJmol^{-1}]	36.33 (30.44)	35.31 (29.70)	33.42 (28.81)	33.53 (28.87)	31.81 (27.37)	32.71 (28.24)
$\|\mu_a\|$[b] [D]	0.52 (0.51)	1.26 (1.28)	0.10 (0.11)	0.58 (0.83)	0.66 (0.58)	0.79 (0.71)
$\|\mu_b\|$ [D]	0.40 (0.33)	0.69 (0.83)	1. 91 (2.07)	1.67 (1.81)	0.29 (0.42)	0.32 (0.44)
$\|\mu_c\|$ [D]	0.71 (0.85)	0.84 (0.80)	0.07 (0.04)	1.42 (1.50)	0.29 (0.31)	1.34 (1.40)
MP2/aug-cc-pVTZ						
D_e[kJmol^{-1}]	37.29	36.27	33.92	34.35		
$\|\mu_a\|$[b] [D]	0.49 (0.48)	1.18 (1.20)	0.13 (0.08)	0.79 (1.05)		
$\|\mu_b\|$ [D]	0.53 (0.47)	0.88 (1.01)	1.79 (1.94)	1.40 (1.51)		
$\|\mu_c\|$ [D]	0.72 (0.86)	0.84 (0.79)	0.13 (0.11)	1.29 (1.35)		
A [MHz]	2481	2483	2864	2753		
B [MHz]	1143	1060	895	931		
C [MHz]	1077	1057	779	843		

[a] BSSE corrected values are given in parentheses. [b] Calculated using the MP2 density; The values calculated using the HF density are given in parentheses. See text for details. [c] Single-point calculation at the MP2/aug-cc-pVTZ level with the optimised geometry at the MP2/6-311++G(d,p) level.

used to monitor its concentration in the sample mixture. Automatic spectral scans were carried out in the frequency region from 3.98–10.2 GHz with 15 cycles and 0.2 MHz step size. Each transition candidate was then measured separately by using an optimised MW excitation pulse length and sufficient averaging cycles for a signal-to-noise ratio better than 10. More than three hundred rotational lines were measured in this frequency region. There are 23 lines which were absent in the expansions of 0.3% FE in He as carrier gas, indicating that they probably originate from the FE···Ne_x complexes. Transitions belonging to the FE monomer (10 lines) and the FE···Ne_x complexes were excluded from further consideration.

The autoscan spectra exhibit an eye-catching pattern with narrowly spaced triplets around 4024, 6036, 8048 and 10060 MHz. They are consistent with *a*-type $J=2$–1, 3–2, 4–3 and 5–4 transitions of a near-prolate top. They were tentatively assigned to the conformer *i*|*c*|*hom*, which has a predicted basis-corrected (BC) of 6 MHz, whereas all others have the BC values of 77 MHz or larger. Another distinct pattern is a group of transitions observed around 4460 MHz. This corresponds to the Q-branch *b*- and *c*-type $K_a=2$–1 transitions with *J* ranging from 2 to 8. They were also assigned to *i*|*c*|*hom*, which was predicted to have *b*- and *c*-dipole moment components of similar magnitude. The observed spectrum in the 4460 MHz region is depicted in Figure 2, together with the simulated spectrum of *i*|*c*|*hom* in this frequency region. Besides *i*|*c*|*hom*, three additional sets of transitions were assigned. Because the predicted rotational constants differ substantially between the compact and the open conformers, it is relatively straightforward to recognise that the additional three sets of rotational constants determined experimentally belong to the other three compact conformers.

While the correlations of the observed rotational constants to those of the *i*|*c*|*het* and *i*|*c*|*hom* predictions were fairly clear, the situation was less evident for *a*|*c*|*het* and *a*|*c*|*hom*, because their predicted rotational constants are more similar. In this case, we also utilised the detailed comparison of the trends of the observed and calculated dipole moment components. For example, the *c*-type transition intensities of *a*|*c*|*het* were optimised experimentally with a much longer MW excitation pulse width than its *b*-type transitions, while the *b*- and *c*-type transitions of *a*|*c*|*hom* were optimised with similar MW excitation pulse widths. This is consistent with the prediction that *a*|*c*|*het* has a *c*-dipole moment component many times smaller than its *b*-component, whereas the *b*- and *c*-dipole moment components of *a*|*c*|*hom* are of similar magnitude. In general,

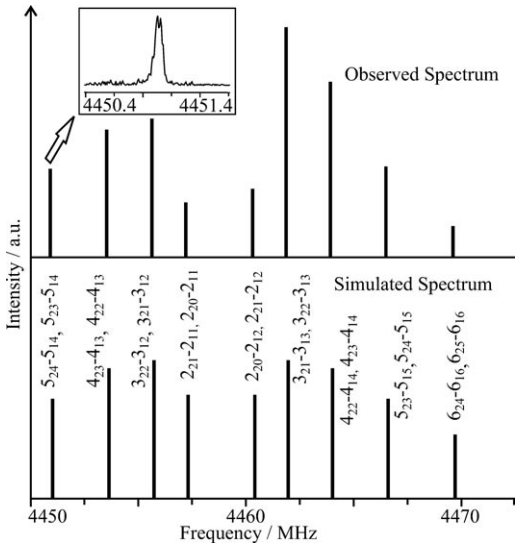

Figure 2. Top: a section of the rotational spectrum of the *i*|*c*|*hom* conformer showing the *b*- and *c*-type transitions with $K_a=2$–1 and *J* ranging from 2 to 6. Transitions observed are represented by sticks with the corresponding experimental intensities. An example showing overlapping *b*- and *c*-type transitions with $J=5$ is given in the insert. Please note that the line width (FWHM) is ~30 kHz, twice the usual line width because of the unresolved Doppler splittings and the overlapping *b*- and *c*-type lines. Bottom: the spectrum simulated from the experimental rotational and centrifugal constants with a rotational temperature of 1 K. The rotational transitions are labelled with J_{KaKc} quantum numbers.

the dipole moment information supports the frequency based conformer assignments discussed above.

Altogether, about 200 pure rotational transitions were unambiguously assigned to four dimeric FE conformers, namely *i*|*c*|*het*, *i*|*c*|*hom*, *a*|*c*|*het*, and *a*|*c*|*hom*. The measured transitions and their spectroscopic assignments are given in Tables S4–S7, available as Supporting Information. The spectroscopic constants obtained from spectroscopic fits using Watson's S-reduction[27] semi-rigid rotor model[28] are listed in Table 2 for all four conformers observed. Also listed in Table 2 are the relative magnitudes of the electric dipole moment components estimated from the experimen-

Table 2. Experimental rotational and centrifugal distortion constants and relative magnitudes of the dipole moment components of the four dimeric FE conformers.

	i|*c*|*het*	*i*|*c*|*hom*	*a*|*c*|*het*	*a*|*c*|*hom*
A [MHz]	2482.7877(3)[a]	2492.3145(9)	2882.0866(6)	2807.4482(4)
B [MHz]	1091.0870(2)	1006.5733(2)	867.1778(2)	883.9286(2)
C [MHz]	1026.2203(2)	1005.5385(2)	753.2254(2)	788.8082(2)
D_J [kHz]	0.897(9)	0.884(3)	0.609(3)	0.871(3)
D_{JK} [kHz]	0.275(9)	0.946(18)	−2.45(1)	1.38(1)
D_K [kHz]	−0.108(37)	−0.378(187)	15.5(1)	5.66(2)
d_1 [kHz]	−0.0071(20)	0.0043(18)	0.0303(17)	−0.0113(18)
d_2 [kHz]	−0.031(1)	0.023(1)	0.0105(4)	−0.0217(5)
κ	−0.9109	−0.9986	−0.8929	−0.9057
N[b]	63	49	27	59
σ[c] [kHz]	2.3	2.8	1.2	2.9
rel. μ[d]	$\lvert\mu_c\rvert > \lvert\mu_a\rvert > \lvert\mu_b\rvert$	$\lvert\mu_a\rvert > \lvert\mu_c\rvert > \lvert\mu_b\rvert$	$\lvert\mu_b\rvert \gg \lvert\mu_c\rvert \approx \lvert\mu_a\rvert$	$\lvert\mu_b\rvert \approx \lvert\mu_c\rvert > \lvert\mu_a\rvert$

[a] The error given in parenthesis in units of the last digits. [b] Number of the rotational transitions fitted. [c] Standard deviation of the fit. [d] Relative strength of the dipole moment components $|\mu_a|$, $|\mu_b|$ and $|\mu_c|$, as estimated from the optimised MW excitation pulse lengths at the $\pi/2$ condition.

tal optimised MW excitation pulse widths. A spectral simulation and fitting program, Jb95,[29] was used to evaluate the rotational temperatures for these conformers, which are about 1 K.

The relative abundances of the four conformers in the jet expansion were estimated from their experimental transition intensities. For simplicity, we used the same *c*-type transitions for *i*|*c*|*het* and *i*|*c*|*hom*, since these transitions were optimised experimentally at similar MW excitation pulse widths, consistent with the fact that their calculated *c*-dipole moment components are quite close (~0.8 D, see Discussion section for details of dipole moment calculations). Similarly, the *b*-type transitions were used for *a*|*c*|*hom* and *a*|*c*|*het*. For comparison of the inserted and associated conformers, different rotational transitions that are close in frequency were used and the corresponding transition line strength and dipole moment component were taken into account. We also used Jb95 to simulate the relative intensity patterns of several transitions of the dimeric FE conformers and estimated their relative abundances. The estimated relative stability ordering, from the most stable to the least, is *i*|*c*|*het*> *i*|*c*|*hom*>*a*|*c*|*hom*>*a*|*c*|*het* and the ratio of the relative population is 17:9:2:1. Assuming a conformational temperature of ~60 K as reported for this type of hydrogen-bonded complexes with a similar experimental setup,[30] the relative energy differences with respect to the global minimum are 0.0, 0.3, 1.1 and 1.4 kJ mol^{-1}, respectively, assuming a Boltzmann distribution. Another way to establish the relative stability ordering is to perform the "Ar test",[14] or simply substitute a lighter carrier gas with a heavier one.[31] Both methods promote collisional relaxation and have been shown to effectively convert the higher-lying hydrogen-bonded or van der Waals conformers to the global minimum. The "Ar test" result performed with the FE dimer gave the same energy ordering as reported above.

Considerable efforts were spent to locate the two remaining conformers, namely *i*|*o*|*het* and *i*|*o*|*hom* in the ~70 unassigned transitions by using Jb95. However, no patterns could be assigned to the *open* conformers. This suggests that only four *compact* dimeric FE conformers are selectively formed under our experimental condition, and the two *open* conformers are probably substantially less stable than the four observed ones. This point will be further discussed in the section below. Some of the unassigned lines are likely to belong to higher FE aggregates such as the FE trimer and FE tetramer, since their line intensities increase much faster with increasing backing pressure than the dimeric FE conformers. Further investigations of these larger aggregates are underway.

Discussions

Stability ordering of the dimeric FE conformers: One of our goals is to examine the effects of inter- and intramolecular hydrogen bonds on the stability of the dimeric FE conformers. As mentioned before, the energy differences between the conformers of the FE monomer are 8 kJ mol^{-1} and higher, based on the MP2/6-311++G(d,p) calculations. The energy differences among the monomeric FE conformers are substantial such that the formation of the dimeric conformers, consisting of the higher lying FE conformers, is energetically and kinetically less favoured. It is therefore not surprising that the most stable dimeric conformers are made of the most stable *G*+*g*−/*G*−*g*+ FE subunits. A similar conclusion was obtained from the lower level MP2/6-311+G* calculations.[13]

To understand the more subtle molecular recognition among the dimeric conformers observed is, however, more challenging. The energy span of the six most stable dimeric conformers built out of the *G*+*g*−/*G*−*g*+ FE subunits is on the order of 2 kJ mol^{-1} or about 10% of the total binding energy at the MP2/6-311++g(d,p) level of theory. The experimental data indicate that *i*|*c*|*het* is the most stable conformer, followed by *i*|*c*|*hom*, *a*|*c*|*hom*, and *a*|*c*|*het*; *a*|*o*|*het* and *a*|*o*|*hom* are bound with even smaller binding energies. The MP2/6-311++G(d,p) calculations without BSSE corrections and with or without ZPE corrections correctly predict that *i*|*c*|*het* is the global minimum, but fail for the rest. Inclusion of BSSE overcorrects the binding energies and wrongly predicts *a*|*c*|*het* as the global minimum. This is probably not surprising, since BSSE tends to overcorrect with relatively small basis sets such as the one used here. We therefore performed the MP2 geometry optimisations using Dunning's correlation-consistent triple-zeta basis set augmented with the diffuse functions, namely aug-cc-pVTZ,[32] for the four compact dimeric FE conformers observed. For comparison, single-point energy calculations at the MP2/aug-cc-pVTZ level with the MP2/6-311++G(d,p) optimised geometries were also performed for all six dimeric conformers. The resulting dissociation energies, rotational constants, and dipole moment components are collected in Table 1. It is gratifying to see that the experimentally observed stability ordering was correctly captured by the MP2/aug-cc-pVTZ//MP2/6-311++G(d,p) and MP2/aug-cc-pVTZ calculations. Even the more subtle chiral recognition preference observed for the heterochiral conformer in the inserted conformers (*i*|*c*|*het* over *i*|*c*|*hom*) and for the homochiral conformer in the associated conformers (*a*|*c*|*hom* over *a*|*c*|*het*) was correctly predicted. Also the predicted energy ordering stays the same with or without BSSE corrections. The BSSE correction with the aug-cc-pVTZ basis set is much smaller than that with the 6-311++G(d,p) basis set; the former contains 598 basis functions, much larger than the latter with 246 basis functions. It appears that the aug-cc-pVTZ basis set with rich diffuse functions is essential for capturing the subtle energy differences that drive the molecular recognition process in the FE dimer.

To analyse the stability ordering of the six most stable dimeric conformers made of the same *G*+*g*−/*G*−*g*+ FE subunits, we divide the contributions to the raw dissociation energy D_e into three parts: E_d^{dist}, E_a^{dist}, and E^{int}. Their values are listed in Table 3. Here, $E_{d/a}^{dist}$ is the so called fragment distortion or deformation energy for the hydrogen-bond donor

Table 3. The calculated donor and acceptor distortion energies and the interaction energies for the six most stable dimeric FE conformers.

	i|*c*|*het*	*i*|*c*|*hom*	*a*|*c*|*het*	*a*|*c*|*hom*	*i*|*o*|*het*	*i*|*o*|*hom*
MP2/aug-cc-pVTZ//MP2/6-311++G(d, p) level of theory						
$E_d^{dist[a]}$ [kJmol^{-1}]	−1.61	−1.42	−1.98	−2.23	−1.86	−2.02
$E_a^{dist[a]}$ [kJmol^{-1}]	−0.52	−1.05	−0.36	−0.35	−0.29	−0.26
$E^{int[a]}$ [kJmol^{-1}]	38.46	37.78	35.77	36.12	33.97	34.98
$D_e^{[a]}$ [kJmol^{-1}]	36.33	35.31	33.42	33.53	32.71	32.71
MP2/aug-cc-pVTZ level of theory						
E_d^{dist} [kJmol^{-1}]	−1.74	−1.54	−2.70	−3.58		
E_a^{dist} [kJmol^{-1}]	−0.41	−0.85	−0.36	−0.39		
E^{int} [kJmol^{-1}]	39.44	38.65	36.97	38.32		
D_e [kJmol^{-1}]	37.29	36.27	33.92	34.35		

[a] An overview of the different energy terms and their relations is presented in the reaction scheme given in Scheme 1. The definitions of the terms are given Equations (1)–(3). The superscripts "monomer" and "dimer" indicate the usage of the optimised geometries in the corresponding monomer or dimer conformations.

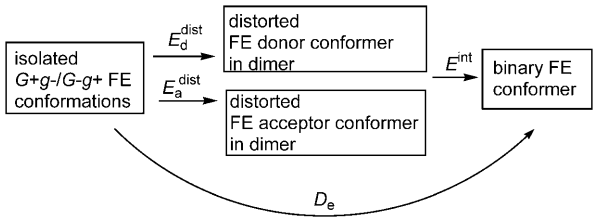

$$E_{d/a}^{dist} = E_{d/a}^{dimer} - E_{FE}^{monomer} \quad (1)$$

$$E^{int} = E_{(FE)_2}^{dimer} - E_d^{dimer} - E_a^{dimer} \quad (2)$$

$$D_e = E_{(FE)_2}^{dimer} - E_{FE}^{monomer} - E_{FE}^{monomer} = E^{int} + E_d^{dist} + E_a^{dist} \quad (3)$$

Scheme 1.

or acceptor, respectively. It corresponds to the energy penalty for distorting the isolated FE conformer from its equilibrium geometry to the optimal geometry in the dimeric FE conformer; E^{int}, the interaction energy of the dimeric complex, is defined in footnote [a] of Table 3, following the notation introduced in references [33,34]. Here, the reference points are the FE donor and acceptor fragments in the dimeric complex. It is clear from Table 3 that the interaction energy is the most significant factor in the relative stability ordering of these six conformers, although the distortion energy term also plays a role. The magnitudes of the donor distortion energy terms are larger than the corresponding acceptor terms in all six cases, implying that the hydrogen-bond donors make greater geometry distortions to fit into the intermolecular hydrogen bonds than the acceptors. It is also interesting and somewhat surprising that the magnitudes of E_d^{dist} are larger in the associated conformers than in the inserted ones, considering that the intramolecular O–H···F interaction has to open up to form the seven-membered intermolecular hydrogen-bond ring in the latter cases. The hydrogen-bond acceptors, on the other hand, show greater distortions in the inserted conformers than in the associated ones. Overall, the inserted conformers are favoured over the associated ones because of their larger interaction energies and smaller distortion penalties.

Geometries of the observed dimeric FE conformers: Good agreement was noted between the calculated and experimental rotational constants with a maximum deviation of 62 MHz or 2% at the MP2/6-311++G(d,p) level. The root mean squares (RMS) of the experimental minus calculated rotational constants for the four observed conformers: *i*|*c*|*het*, *i*|*c*|*hom*, *a*|*c*|*het*, and *a*|*c*|*hom*, are 12, 7, 15, and 36 MHz, respectively, at the MP2/6-311++G(d,p) level. From this, we can infer that the actual geometries of these conformers are very close to the predicted ones given in Figure 1 and in Table S3 in the Supporting Information. The RMS at the MP2/aug-cc-pVTZ level are 42, 43, 24, and 54 MHz, respectively, slightly worse than those obtained with the 6-311++G(d,p) basis set. The superior performance of 6-311++G(d,p) in geometry predictions had been reported before.[17,18,21,22]

Another quantity obtained from the experiments and the calculations is the electric dipole moment component. It was reported that the MP2 density predicts the electric dipole moment components more accurately than the HF density.[35] For comparison, we applied both the HF and MP2 density to calculate the dipole moments using 6-311++G(d,p) and aug-cc-pVTZ. The HF density is the default setting and the usage of the MP2 density was evoked by adding DENSITY=CURRENT in the route section in Gaussian 03.[36] These values are also summarised in Table 1. The differences in the dipole moment components obtained with different densities and basis sets in Table 1 are small. In particular, the MP2 density calculations with the MP2/6-311++G(d,p) geometries provide the best agreements with the experimental data. For example, the *b*-component of *i*|*c*|*hom* was predicted to be slightly larger than the *c*-component at the MP2/aug-cc-pVTZ level of theory, while the opposite was observed. The MP2 density calculations at the MP2/6-311++G(d,p) and MP2/aug-cc-pVTZ//MP2/6-311++G(d,p) level of theory, on the other hand, predicted the same trend as observed experimentally. This may be due to the fact that the MP2/6-311++G(d,p) geometries are closer to the experimental ones. In summary, the comparison of the experimental and calculated dipole components supports the assignment of the four distinct conformers based on the rotational constants discussed previously.

Comparison with the previous studies of the FE and ethanol dimers: The current high-resolution FTMW experiments provide unambiguous identification of the four dimeric FE conformers, which were tentatively assigned in the previous low-resolution jet-cooled FTIR investigation.[13] The current study also supports the previous conclusion that *i*|*c*|*het* is

the most stable dimeric FE conformer. By using the experimentally determined rotational constants of each individual conformer, the corresponding geometries were confirmed directly. Because the rotational transitions of each conformer are well resolved, we can monitor the intensity variations in each conformer separately without the complication of spectral overlapping reported in reference [13]. Additionally, the intensity variation with the "Ar test" is much more dramatic with the pinhole-pulsed FTMW experiments than with the slit-jet FTIR experiments. Therefore minor energy differences that do not cause noticeable changes in the jet FTIR spectra can be detected in a FTMW experiment. This allowed us to establish the stability ordering of the four observed dimeric conformers experimentally.

The related dimeric ethanol conformers were studied previously using FTMW spectroscopy.[16] The fluorination of ethanol increases the number of monomer conformations from three to nine. In addition, the energy span among the monomeric conformers increases from 0.5 kJ mol^{-1} for ethanol[37] to 10.3 kJ mol^{-1} for FE. This is because fluorination at the α-H position of ethanol enables the strong O−H···F intramolecular hydrogen bond, which provides extra stability for the $G+g-/G-g+$ conformations. As a result, the dimeric FE conformers display improved conformational selectivity and flexibility. In particular, the most stable dimeric FE conformers are made exclusively of the lowest energy FE monomer subunit, while the lowest energy dimeric ethanol conformers do not show such preference. In other words, the energy differences among the FE conformers are a major factor in determining the stability ordering of the dimeric FE systems. Fluorination also provides an additional binding site for the hydroxyl group of the hydrogen-bond donor and thus enables the more stable inserted intermolecular hydrogen-bond pattern. The ethanol dimer, in contrast, can only form the associated-type intermolecular hydrogen bonds. Such enhancement of molecular recognition ability upon fluorination has also been detected and analysed in other complexes such as the propylene oxide–FE dimer.[18]

Conclusions

The molecular self-recognition in the dimeric FE conformers has been investigated by using FTMW spectroscopy complemented with high-level ab initio calculations. Rotational spectra of four out of the six most stable dimeric conformers predicted have been recorded and unambiguously assigned. The rotational spectra reveal that the transient chiral FE moiety remains in its favoured $G+g-/G-g+$ conformations in the four dimeric conformers observed. The stability ordering of the dimeric FE conformers has been established experimentally. The heterochiral combination is preferred in the inserted conformers, whereas the homochiral one is favoured in the associated conformers. The trends of the general energy ordering and the subtle chiral recognition were reproduced with MP2 calculations using the aug-cc-pVTZ basis set. Fluorination of ethanol enhances the molecular recognition ability of FE as compared to ethanol by providing additional binding sites for both intra- and intermolecular hydrogen bonds.

Experimental Section

Experimental methods: FE (97%, Sigma–Aldrich) was used without further purification. The samples used are 0.3% FE in Ne (99.9990%, Praxair) or mixtures of 20% Argon (99.996%, Praxair) and 80% He (99.996%, Praxair). The samples were expanded through a pulsed jet pinhole nozzle (General Valve Series 9) with a home made cap (0.8 mm diameter opening and 3.0 mm long exit channel) into the vacuum chamber of a Balle–Flygare type[38] FTMW spectrometer. The spectrometer is described in detail elsewhere.[39] FE and Ne were mixed in several gas cylinders with a total volume of ~4 L so that the optimum stagnation pressure around 3–4 bar was maintained over the long automated survey scans. Rotational lines in the frequency region of 3.9–13 GHz were recorded. The full line width at half maximum is 15 kHz for a well-resolved transition and the accuracy of the frequency determination was estimated to be 2–3 kHz. Each transition appeared as a Doppler doublet, because the propagation direction of the microwave radiation was parallel to the molecular expansion. The central frequency was obtained by unweighted averaging of the frequency pair.

Computational methods: MP2 geometry optimisation calculations with the 6-311++G(d,p) and the aug-cc-pVTZ[32] basis set were performed using the Gaussian 03 suite of programs.[36] Stationary points were confirmed to be local minima by harmonic frequency analyses. The BSSE corrections were determined using the counterpoise correction methods of Boys and Bernardi[25] in the same way as suggested in reference [33].

Acknowledgements

This research was funded by the University of Alberta, the Natural Sciences and Engineering Research Council of Canada, the Canada Foundation for Innovation (New Opportunity) and Alberta Ingenuity (New Faculty Award and New Faculty Extension Award). We thank W. Jäger for the instrument time on the microwave spectrometer and the Academic Information and Communication Technology group at the University of Alberta for access to the computing facilities. We are grateful to T. Scharge, C. Emmeluth, T. Häber, and M. A. Suhm for kindly providing detailed information about their investigation of the dimeric FE conformers. N.B. thanks Alberta Ingenuity and the German Academic Exchange Service (DAAD) for postdoctoral fellowships.

[1] K. Gast, A. Siemer, D. Zirwer, G. Damaschun, *Eur. Biophys. J.* **2001**, 30, 273–283, and references therein.
[2] M. Buck, *Q. Rev. Biophys.* **1998**, *31*, 297–355.
[3] K. A. Bolin, M. Pitkeathly, A. Miranker, L. J. Smith, C. M. Dobson, *J. Mol. Biol.* **1996**, *261*, 443–453.
[4] a) D.-P. Hong, M. Hoshino, R. Kuboi, Y. Goto, *J. Am. Chem. Soc.* **1999**, *121*, 8427–8433; b) A. Berkessel, J. A. Adrio, D. Hüttenhain, J. M. Neudörfl, *J. Am. Chem. Soc.* **2006**, *128*, 8421–8426.
[5] A. Jasanoff, A. R. Fersht, *Biochemistry* **1994**, *33*, 2129–2135.
[6] N. Schönbrunner, J. Wey, J. Engels, H. Georg, T. Kiefhaber, *J. Mol. Biol.* **1996**, *260*, 432–445.
[7] D. Roccatano, G. Colombo, M. Fioroni, A. E. Mark, *Proc. Natl. Acad. Sci. USA* **2002**, *99*, 12179–12184.
[8] I. Bako, T. Radnai, M. C. B. Funel, *J. Chem. Phys.* **2004**, *121*, 12472–12480.
[9] T. Takamuku, T. Kumai, K. Yoshida, T. Otomo, T. Yamaguchi, *J. Phys. Chem. A* **2005**, *109*, 7667–7676.
[10] H. Reiersen, A. R. Rees, *Protein Eng.* **2000**, *13*, 739–743.
[11] T. Scharge, T. Häber, M. A. Suhm, *Phys. Chem. Chem. Phys.* **2006**, *8*, 4664–4667.

[12] T. Scharge, C. Cézard, P. Zielke, A. Schütz, C. Emmeluth, M. A. Suhm, *Phys. Chem. Chem. Phys.* **2007**, *9*, 4472–4490.
[13] a) T. Scharge, C. Emmeluth, T. Häber, M. A. Suhm, *J. Mol. Struct.* **2006**, *786*, 86–95; b) T. Scharge, T. N. Wassermann, M. A. Suhm, *Z. Phys. Chem.* **2008**, *222*, 1407–1452.
[14] C. Emmeluth, V. Dyczmons, T. Kinzel, P. Botschwina, M. A. Suhm, M. Yanez, *Phys. Chem. Chem. Phys.* **2005**, *7*, 991–997.
[15] M. E. Sanz, V. Cortijo, W. Caminati, J. C. López, and J. L. Alonso, *Chem. Eur. J.* **2006**, *12*, 2564–2570.
[16] J. P. I. Hearn, R. V. Cobley, B. J. Howard, *J. Chem. Phys.* **2005**, *123*, 134324.
[17] N. Borho, Y. Xu, *Angew. Chem.* **2007**, *119*, 2326–2329; *Angew. Chem. Int. Ed.* **2007**, *46*, 2276–2279.
[18] N. Borho, Y. Xu, *J. Am. Chem. Soc.* **2008**, *130*, 5916–5921.
[19] J. S. Binkley, J. A. Pople, *Int. J. Quantum Chem.* **1975**, *9*, 229–236.
[20] R. Krishnan, J. S. Brinkley, R. Seeger, J. A. Pople, *J. Chem. Phys.* **1980**, *72*, 650–654.
[21] L. B. Favero, B. M. Giuliano, S. Melandri, A. Maris, W. Caminati, *Chem. Eur. J.* **2007**, *13*, 5833–5837.
[22] a) Z. Su, Q. Wen, Y. Xu, *J. Am. Chem. Soc.* **2006**, *128*, 6755–6760; b) Z. Su, Y. Xu, *Angew. Chem.* **2007**, *119*, 6275–6278; *Angew. Chem. Int. Ed.* **2007**, *46*, 6163–6166.
[23] K. S. Buckton, R. G. Azrak, *J. Chem. Phys.* **1970**, *52*, 5652–5655.
[24] a) D. Green, S. Hammond, J. Keske, B. H. Pate, *J. Chem. Phys.* **1999**, *110*,1979–1989; b) D. A. McWhorter, E. Hudspeth, B. H. Pate, *J. Chem. Phys.* **1999**, *110*, 2000–2009.
[25] S. F. Boys, F. Bernardi, *Mol. Phys.* **1970**, *19*, 553–566.
[26] C. L. Brummel, S. W. Mork, L. A. Philips, *J. Chem. Phys.* **1991**, *95*, 7041–7053.
[27] J. K. G. Watson in *Vibrational Spectra and Structure: A series of Advances, Vol. 6* (Ed.: J. R. Durig), Elservier, New York/Amsterdam, **1977**, pp. 1–78.
[28] V. Typke, "Program ZFAP6 ", to be found under http://www.Uni-ulm.de/~typke/progbe/zfap6.html, **2002**.
[29] a) David F. Plusquellic, **2002**, User Guide to the Jb95 Spectral Fitting Program, (version 2.00.3), to be found under http://physics.nist.-gov/jb95, National Institute of Standards and Technology, Gaithersburg, MD; b) D. F. Plusquellic, R. D. Suenram, B. Mate, J. O. Jensen, A. C. Samuels, *J. Chem. Phys.* **2001**, *115*, 3057–3060.
[30] N. Borho, Y. Xu, *Phys. Chem. Chem. Phys.* **2007**, *9*, 4514–4520.
[31] Z. Su, N, Borho, Y. Xu, *J. Am. Chem. Soc.* **2006**, *128*, 17126–17131.
[32] T. H. Dunning Jr. , *J. Chem. Phys.* **1989**, *90*, 1007–1023.
[33] S. S. Xantheas, *J. Chem. Phys.* **1996**, *104*, 8821–8824.
[34] K. Szalewicz, B. Jeziorski, *J. Chem. Phys.* **1998**, *109*, 1198–1200.
[35] K. L. Bak, J. Gauss, T. Helgaker, P. Jørgensen, J. Olsen, *Chem. Phys. Lett.* **2000**, *319*, 563–568.
[36] Gaussian 03, Revision E.01, M. J. Frisch, G. W. Trucks, H. B. Schlegel, G. E. Scuseria, M. A. Robb, J. R. Cheeseman, J. A. Montgomery, Jr., T. Vreven, K. N. Kudin, J. C. Burant, J. M. Millam, S. S. Iyengar, J. Tomasi, V. Barone, B. Mennucci, M. Cossi, G. Scalmani, N. Rega, G. A. Petersson, H. Nakatsuji, M. Hada, M. Ehara, K. Toyota, R. Fukuda, J. Hasegawa, M. Ishida, T. Nakajima, Y. Honda, O. Kitao, H. Nakai, M. Klene, X. Li, J. E. Knox, H. P. Hratchian, J. B. Cross, V. Bakken, C. Adamo, J. Jaramillo, R. Gomperts, R. E. Stratmann, O. Yazyev, A. J. Austin, R. Cammi, C. Pomelli, J. W. Ochterski, P. Y. Ayala, K. Morokuma, G. A. Voth, P. Salvador, J. J. Dannenberg, V. G. Zakrzewski, S. Dapprich, A. D. Daniels, M. C. Strain, O. Farkas, D. K. Malick, A. D. Rabuck, K. Raghavachari, J. B. Foresman, J. V. Ortiz, Q. Cui, A. G. Baboul, S. Clifford, J. Cioslowski, B. B. Stefanov, G. Liu, A. Liashenko, P. Piskorz, I. Komaromi, R. L. Martin, D. J. Fox, T. Keith, M. A. Al-Laham, C. Y. Peng, A. Nanayakkara, M. Challacombe, P. M. W. Gill, B. Johnson, W. Chen, M. W. Wong, C. Gonzalez, J. A. Pople, Gaussian, Inc., Wallingford CT, **2004**.
[37] A. Zehnacker, M. A. Suhm, *Angew. Chem.* **2008**, *120*, 7076–7100; *Angew. Chem. Int. Ed.* **2008**, *47*, 6970–6992.
[38] a) T. J. Balle, W. H. Flygare, *Rev. Sci. Instrum.* **1981**, *52*, 33–45; b) U. Andresen, H. Dreizler, J.-U. Grabow, W. Stahl, *Rev. Sci. Instrum.* **1990**, *61*, 3694–3699.
[39] Y. Xu, W. Jäger, *J. Chem. Phys.* **1997**, *106*, 7968–7980.

Received: October 1, 2008
Published online: November 28, 2008

